Improvement of knowledge and modelling of heat transfer in cryogenic combustion chambers

Lucien Vingert, Philippe Grenard*, Gérard Ordonneau*,*
*Stéphane Petitot**, Sandrine Palerm***
**ONERA, The French Aerospace Lab, Chemin de la Hunière et des Joncherettes,*
BP 80100 FR-91123 PALAISEAU CEDEX
***CNES, Launcher Directorate*
52 rue Jacques Hillairet 75612 PARIS CEDEX 12

Abstract

In order to improve the knowledge of heat transfer in cryogenic rocket engines, as well as to assess modelling capabilities to reproduce it, CNES and ONERA decided to build a high pressure - high mixture ratio subscale combustion chamber, fed with five coaxial injectors disposed in a cross pattern, able to reproduce representative liquid rocket engines conditions (CONFORTH project). After a maiden hot run in 2010, further test series with both gas/gas and liquid/gas injection were run in 2012-2014 to increase the database with new heat fluxes measurements and visualizations of the flame and the atomizing jet. In the meantime, computations were performed using the ONERA in-house code CEDRE on the tested configurations.

The combustor is quickly presented along with experimental results obtained during the latest campaigns. The measurement are compared, analyzed and reduced to give a first set of data for simulation. The numerical procedure is quickly reminded and numerical results obtained for the different cases are compared to experimental data.

The numerical results are in good agreement with experimental data, despite some uncertainties on the fluxes compare to temperature. Nevertheless, the good comparison between numerical results and experimental measurements give confidence in the methodology and point out some improvements to introduce.

1. Introduction

The quest for high performance of rocket engines, using bleed or expander cycles as RL10, LE-5 or Vinci engines, and the possible needs of reusable engines as for future launchers request a precise knowledge and a mastering of the power's source of the engine, that is heat fluxes through the thin walls of the combustion chamber separating the hot combustion gases from the fluid flowing through the cooling circuit. Indeed, in the case of expander cycle, the function of the cooling circuit is not only to cool the chamber but also to extract the power needed to drive the turbines. The higher the power, higher the wall temperature and the thermal constraints in the material are. Thus, in order to be able to define the "exactly need design", and so on to reduce the mass of the motor, and moreover to insure the reuse of an engine, margins must be adequately defined. Thus, accurate prediction of wall heat fluxes appears to be of primary importance for liquid propellant rocket engine (LPRE) design because it directly influences the life-cycle of the combustion chamber. In this field, a trial-and-error design methodology suffers from high costs and does not give a fundamental understanding of the physical processes involved.

Hopefully, during the last decade, progresses in Computational Fluid Dynamics (CFD) and high performance computing (HPC) have gained in maturity and allow nowadays methodology for multiphysics simulation of a rocket engine with a detailed representation and simulation of different physical processes [1],[2],[3].

Nevertheless, LPRE simulations remain difficult to validate because of the difficulty to obtain a complete set of experimental data, linked to the fact that obtaining quantitative measurements in the extreme thermodynamic conditions encountered in LPRE is still a major hurdle. Numerical codes need to be validated on well-known configurations. Some attempts have been done on part of the whole system, mainly the regenerative cooling channels [4],[6] where, for instance, Quering et al. study the influence of curvature on the heat transfer. But detailed experimental studies of cryogenic propellant combustion, in well controlled and nevertheless representative operating conditions, remain requested.

Therefore ONERA and CNES decided, in 2006, to build a new combustor (Bhp-HrM for Boîtier haute pression – Haut rapport de Mélange in French), water-cooled and fed with multiple (five) injectors of various types in the framework of a project named CONFORTH (CONception et Fabrication d'un bOîtier refroidi et d'une Tuyère à Haut rapport de mélange, in French) and operated on the ONERA cryogenic test bench named "Mascotte" ([13],[14]). One of the goals was to acquire a sufficient aero-thermal database for both the thrust chamber and the nozzle. That is why more than 200 thermocouples were implemented in the wall and at the injection backplane of the combustor, distributed along three generating lines, taking into account as much as possible of the symmetries in the configuration. A first campaign was successfully held in 2010 [9], during which the chamber was fed with gaseous oxygen and hydrogen. The combustor successfully worked in an extended domain varying from 2 to 6,5 MPa for the pressure and from 2 to 7 for the mixture ratio MR. Heat fluxes for the different parts of the combustor, as well as adiabatic temperatures and heat transfer coefficients for the face plate, have been deduced from temperature measurements, leading to a database which already helps to consolidate the design procedure and will later be used for CFD validation, including simulation of the heat transfer at the walls [8],[11].

Further test series with both gas/gas and liquid/gas injection were run in 2012-2014 to increase the database with new heat fluxes measurements and visualizations of the flame and the atomizing jet [4],[15]. In the meantime, computations on the tested configurations were performed.
This paper will present the improvement of knowledge and modelling of heat transfer in cryogenic combustion chambers obtained during the last two years. It is organized as follows; first the combustor is quickly presented along with experimental results obtained during the latest campaigns. The measurements are compared, analyzed and reduced to give a first set of data for simulation. So, the numerical procedure is quickly reminded and numerical results obtained for the different cases are compared to experimental data.

2. Experimental results

Experimental investigations of wall heat fluxes started in 2010 on the Mascotte cryogenic test facility of ONERA. The bench itself, as well as the water-cooled combustion chamber used for these tests have been described in several papers [7],[8],[3],[10], and will not be described here again. Let us just recall that several versions of the hardware were developed and manufactured for the different items of interest in experimental research. The first one is the "thermal" version (Fig. 1a) used in the present study; it consists of an injection head with an interchangeable face plate (instrumented non-cooled or non-instrumented non-cooled or non-instrumented water cooled), two ferrules, water cooled and equipped with thermocouples along three generating lines, and an axi-symmetric nozzle. In the second version (Fig. 1b), devoted to optical diagnostics, the first ferrule is replaced by a visualization module with four optical ports. Five coaxial injectors are used to feed the chamber with oxygen/hydrogen mixtures. The hydrogen is always injected gaseous at a temperature varying from ambient down to 100 K, while the oxygen can be gaseous at room temperature or liquid at approximately 90 K. The operational domain covers a large range of pressures, from subcritical to supercritical (1 to 7 MPa), as well as a large variety of mixture ratios from 1 to 7, allowing investigations of both gas generator and thrust chamber applications.

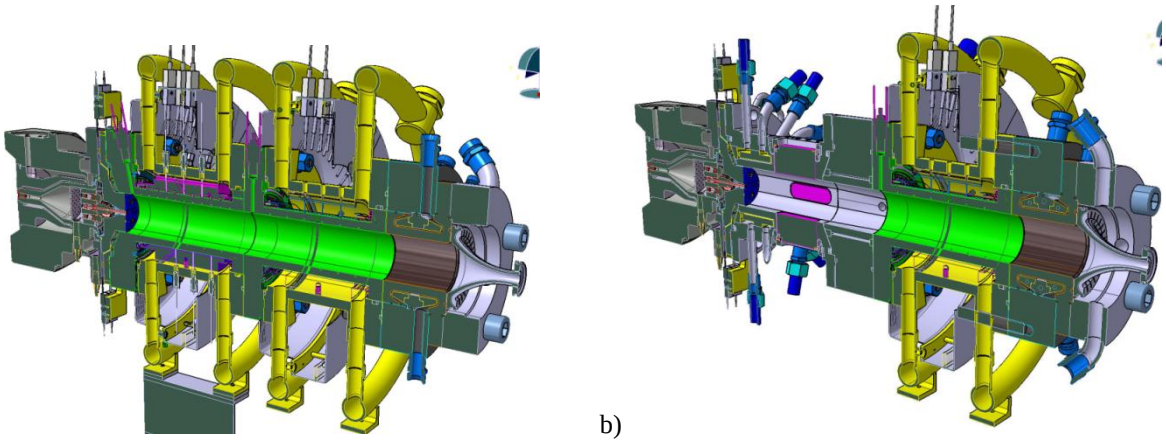

a) b)

Figure 1 – The water-cooled combustion chamber.

During the first test series presented at EUCASS 2011 [9], only gas/gas tests were achieved. Further test series with both gas/gas and liquid/gas injection were run in 2012-2014 to increase the database with new heat fluxes measurements and visualizations of the flame and the atomizing jet [10],[15].

The achieved operating points of the short duration tests are located in the (mixture ratio, chamber pressure) plane on Figure 2, where the expected dimensionless heat flux are represented by the color scale. The expected values were computed with a classical Colburn correlation, using the adiabatic combustion temperature for the hot gases at each operating point. One major goal of these campaigns was to check the validity of these predicted values, and therefore to evaluate precisely the heat fluxes on the different parts of the motor, i.e. along the cylindrical part and on the injection plate. For the first one, the heat fluxes can be derived from a spatial gradient between two thermocouples located near the walls (one on the hot gas side and the other on the cooling water side) due to the high conductivity of the copper alloy. The model is the same as the one used in 2010 (see [3]). It is based on the assumption that longitudinal and azimuthal components of the fluxes are small compared to their radial one. We consider the diffusion of heat through the wall and use the difference in temperature between the cold and hot sides to extract heat fluxes: this method is completely valid as soon as thermal steady state is reached, i.e. as soon as the temperature becomes stationary.

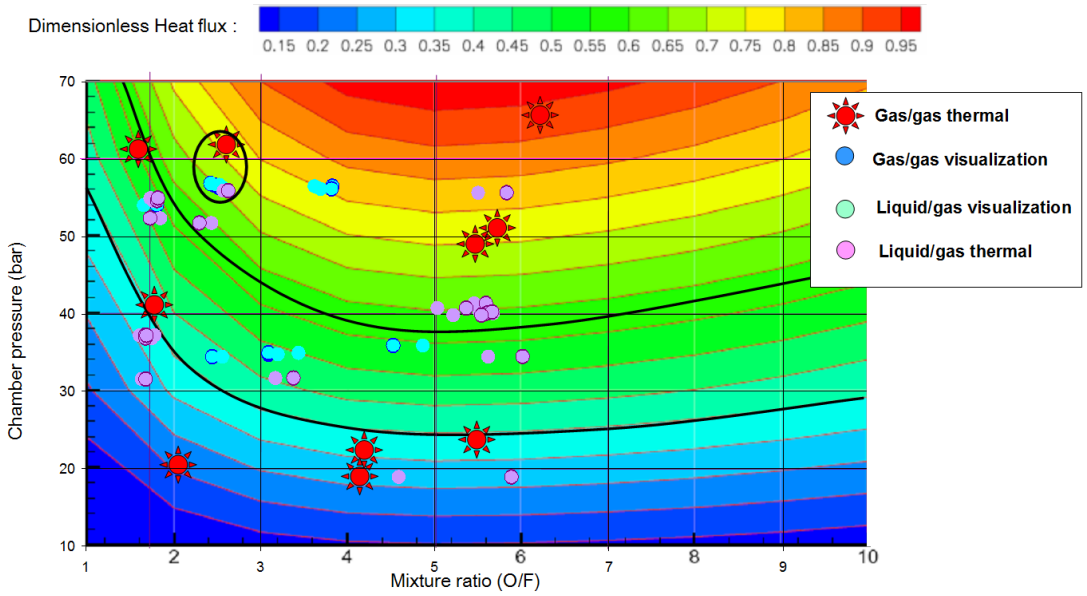

Figure 2 – Achieved operating points of the different test series.

Among the different operating points reached during the successive campaigns, there are three tests, surrounded by a black ellipse on figure 2, which are sufficiently close to each other, to allow a comparison between the three experimental conditions, thermal version of the combustor operated in gas/gas, visualization version of the combustor operated in liquid/gas and finally thermal version operated in liquid/gas.
Figures 3 and 4 show that the temperatures and fluxes observed on the cylindrical parts in gas/gas and liquid/gas conditions are of the same order of magnitude but the time evolution was much smoother in gas/gas operation. It may also be noticed that the highest observed temperatures are slightly higher in the first part of the chamber and slightly lower in the second part for the liquid/gas case as compared to the gas/gas case. This indicates that the flame is probably shorter in the liquid/gas case, which is due to a better mixing because the coaxial element is not the best choice for gas/gas propellants. The comparison between the thermal and visualization tests shows that the temperatures and fluxes on the second ferrule are also similar (Figure 5).
Temperatures measured in the cooling water circuit of the ferrule 1 during the two thermal campaigns were also compared (Figure 6). It appears once more that the levels are similar, but that these temperatures, similarly to all the other ones are heckled in liquid/gas conditions and much smoother in gas/gas conditions.
Figure 7 shows the same measurements at time t = 34 s, that is to say in the steady state. It is observed that in both cases, temperatures plotted versus the thermocouple number, which is actually versus the distance to the injection plate, are sawtooth-shaped, although the ferrule has been refurbished between the two campaigns. It is important to note that the 6 thermocouples TCR identified as being mounted along a generating line of the ferrule 1 could not

practically be on the same generating line and that for each of the planes, odd TCRs are located near the walls thermocouples (TPG TPE) while peer TCRs are diametrically opposed. We have here evidence, even in the cooling channels, that the assumption of axisymmetric flow may be somewhat in default.

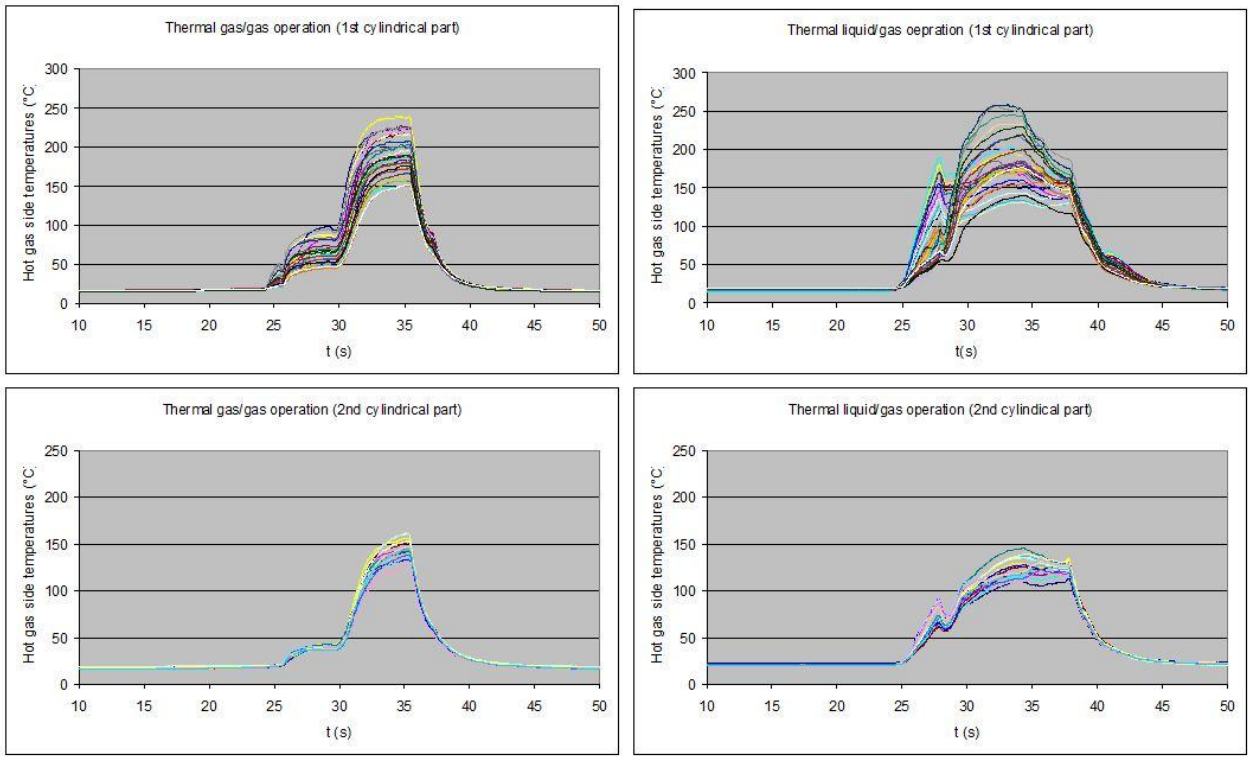

Figure 3 – Temperatures of the hot gas side for gas/gas and liquid/gas operation in the thermal configuration.

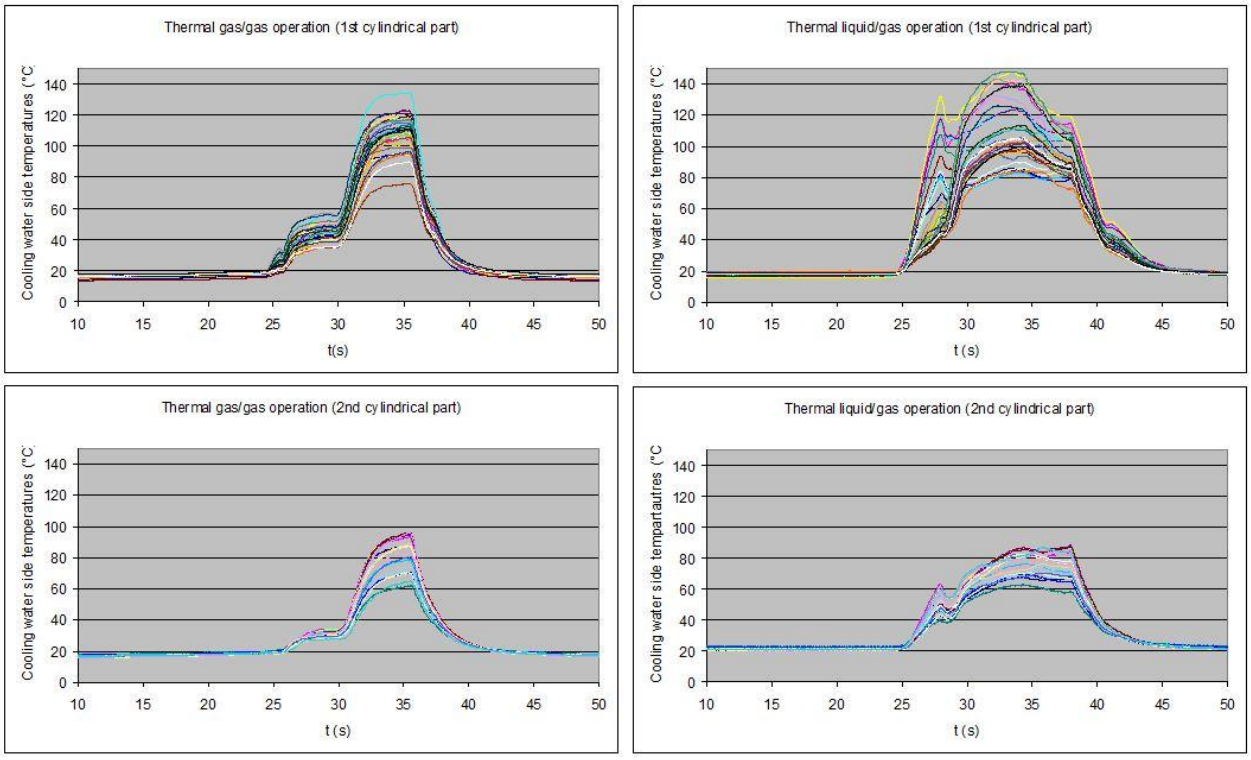

Figure 4 – Temperatures of the cooling water side for gas/gas and liquid/gas operation in the thermal configuration.

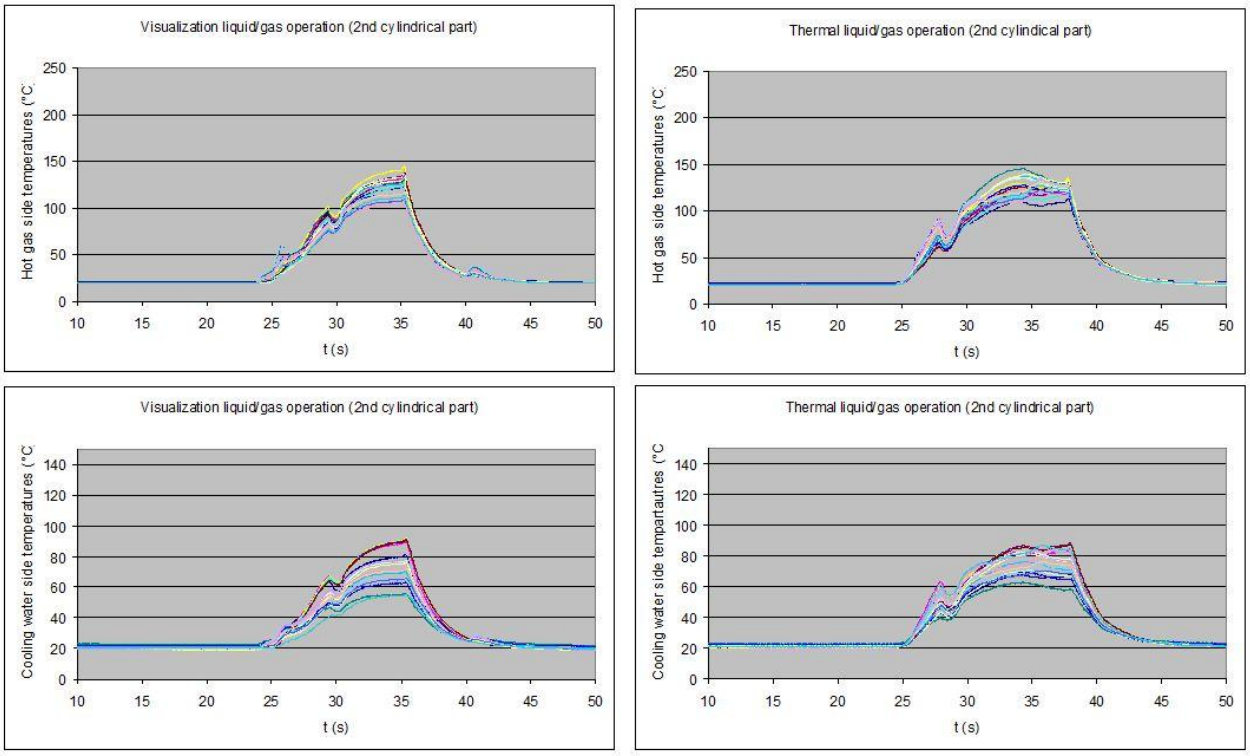

Figure 5 – Temperatures for liquid/gas operation in the visualization and thermal configurations.

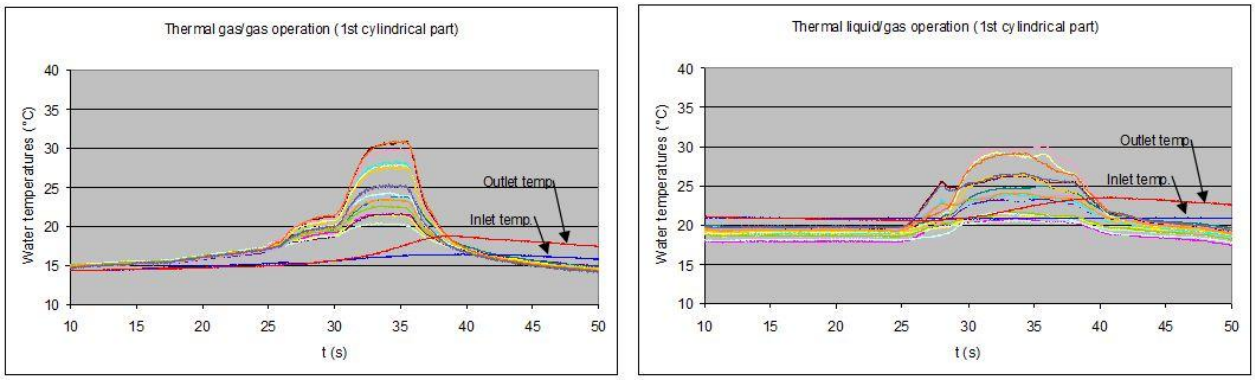

Figure 6 – Temperatures of the cooling water for gas/gas and liquid/gas operation in the thermal configuration.

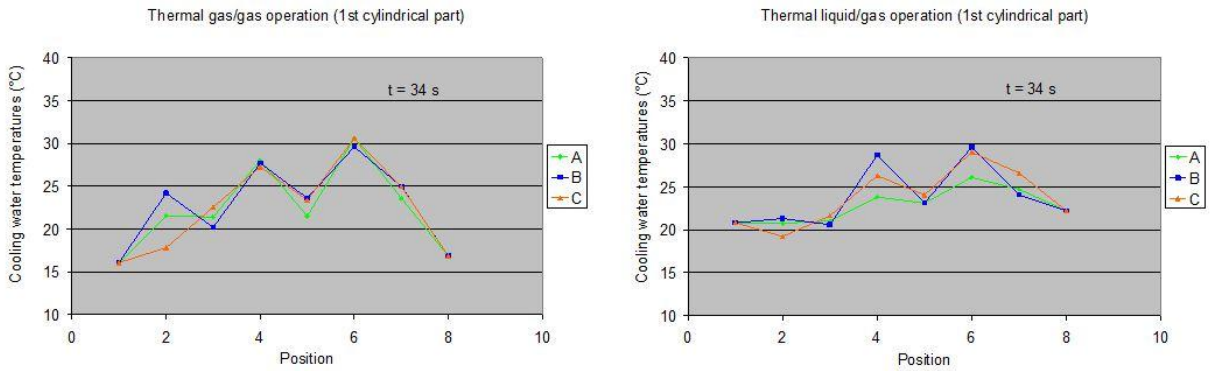

Figure 7 – Temperatures of the cooling water for gas/gas and liquid/gas operation in the thermal configuration.

The gas/gas thermal configuration case of these three tests has been numerically simulated. The result of this computation and the comparison to the experimental results is the topic of the next paragraph.

3. Experimental data treatment

Experimental data is obtained as thermocouples temperatures. From these temperatures, a heat flux is extracted by an analytical solution of stationary conduction problem in cylindrical coordinates:

$$\phi_{ch} = \frac{\lambda(T_H - T_C)}{r_{ch}\ln(r_H/r_C)}$$

where "H" subscript represent the **H**ot (combustion gases side) measurement radius, "C" the **C**old (water cooling side) measurement radius and "ch" the combustion **ch**amber wall.
Due to the small relative difference in radiuses, this equation is very close to:

$$\phi_{ch} = \frac{r_H}{r_{ch}}\frac{\lambda(T_H - T_C)}{(r_H - r_C)}$$

Thus, an a priori estimation of the uncertainties of the heat fluxes evaluation is given by:

$$\frac{\Delta\phi}{\phi} = \frac{\Delta r_H}{r_H} + \frac{\Delta r_{ch}}{r_{ch}} + \frac{\Delta(T_H - T_C)}{T_H - T_C} + \frac{\Delta(r_H - r_C)}{r_H - r_C}$$

The two first terms are negligible due to the size of the radiuses compared to the precision of manufacturing; the third term is evaluated to be variable, depending on the measurements, and the last term, corresponding to the uncertainties linked to the position of the sensors, is estimated to be about 6%.
A first, rough, estimation of the temperature uncertainties is computed by evaluating the mean value and standard deviation of the 3 measurement lines. We believe that the uncertainties evaluated by this treatment are overestimated, especially on the first ferrule because those 3 lines of sensors does not share the same physics (one of them is aligned with a "side" injector, another one is exactly between two side injectors and the last one is at a position in-between), which leads to physical differences which are considered to be measurement uncertainties by this treatment. On the second ferrule, the flames are mixed and a quasi-homogeneous flow is obtained. Different reflections and procedures are currently undertaken to lower those uncertainties.
One must keep in mind that the evaluation of the heat fluxes is derived from the temperature measurements, and, as such, this a posteriori evaluation exhibits higher uncertainties than the temperature one.

4. Numerical simulation

The last two years were also used to perform first computations on these configurations, based on the data obtained during 2010 campaign (gaseous O2 – gaseous H2) [8] and following a methodology developed in 2011 – 2012 [11]. The procedure is quickly reminded and numerical results obtained are compared to experimental data.

4.1 Numerical procedure

The geometry is built upon two domains presented in Figure 8, a fluid one (blue) and a solid one (grey). The fluid domain, representing the combustion chamber, is made of a central injector and 4 surrounding injectors, and it is closed by a convergent-divergent nozzle. The solid domain is made of cylindrical walls where, experimentally, a liquid water film is flowing along the external part of that domain. By symmetry, the effective domain computed is restrained to a quarter of the full geometry.

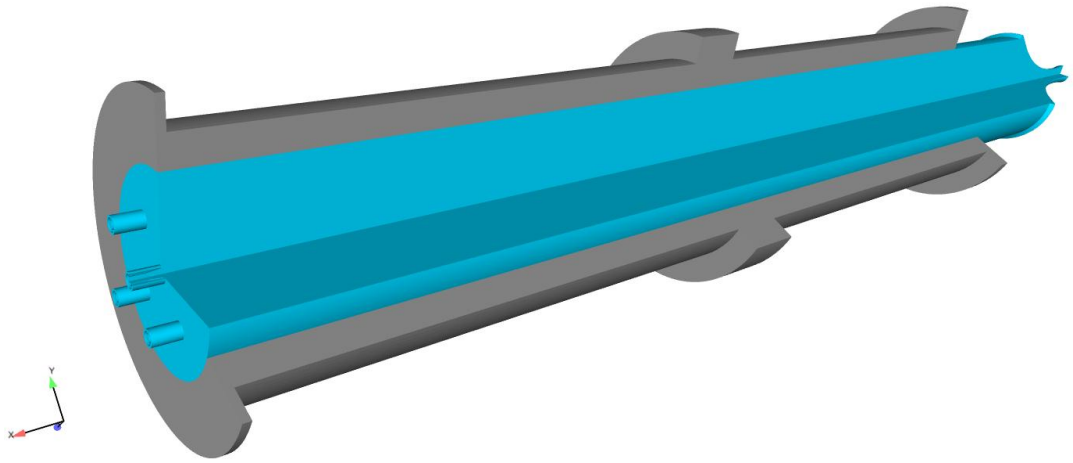

Figure 8 – Illustration of the solid and fluid physical domains.

The numerical procedure is based on RANS computations, with thermal coupling with the solid wall surrounding the combustion chamber. The computations are carried out using in-house energetics code CEDRE [16] for both the reactive, turbulent fluid flow and the solid conduction problem.
The solid domain is defined as a copper alloy, with thermal conductivity depending on temperature. Since only the steady state solution is looked for, the specific heat of the material is specified constant as its evolution with the temperature is only important for transient evolution.
The fluid flow computation is carried out with the following modelling:

- RANS k-ω SST turbulent model [8] with linear eddy viscosity model (Boussinesq, Fourier),
- Turbulent combustion model with relaxation to equilibrium: the mass source of a species "*i*" is given by the equation $\dot{\omega}_i = C\rho(Y_i - Y_i^{eq})/\tau_t$ with τ_t being the turbulent time scale, C a model constant (of the order of unity). This model exhibits high robustness compared to chemical kinetics and a correct equilibrium behaviour compared to only one complete, irreversible reaction used in classical simple turbulent combustion model such as EBU or CFM models,
- Low Reynolds approach for the combustion chamber walls.

The boundary conditions of the computation consist of:

- Prescribed mass flow rates and temperatures of propellants injected in the combustion chamber,
- Supersonic flow at the exit of the choked nozzle closing the combustion chamber,
- At the hot side wall of the ferrule :
    - No-slip conditions for the flow,
    - Temperature of the wall imposed by thermal coupling with the solid domain,
- At the cold side wall, the experimental temperature map measured on the cold side of the ferrule wall is imposed for the external boundary condition of the solid domain.

4.2 Computed Operating Points

The main goal of the study is to assess our capability to evaluate correctly both temperature and heat fluxes at the combustion chamber wall for different operating points. Thus, three different operating points were computed, as presented in Table 1.

Table 1 - Operating points computed.

Denomination	Mixture ratio (mO_2/mH_2)	Velocity ratio (VH_2/VO_2)	Chamber Pressure (bar)
M7P60	7.15	1.4	66
M3P60	3.2	3.0	60
M2P40	1.9	5.6	41

The choice of these points follow two objectives: the first one is to compute a dimensioning point, with high mixture ratio and high pressure, leading to maximum heat fluxes. The second objective is to evaluate the methodology at different location (in the (P,M) map) as well as to evaluate the effect of a varying velocity ratio between hydrogen and oxygen flows. Moreover, the pressure obtained on the two first points here is above the critical pressure of both

components, leading to supercritical operating points. As the temperature of injection is however ambient, those points are not transcritical and, as such, they are easier to compute.

4.3 Results and discussion

The dimensionless temperature (θ), expressed as a function of the measured temperature so that it varies between 0 and 1 for all cases, allows comparison between the different operating points. The advantage of the coupled computation is to permit direct comparison of measured and computed values of temperature instead of performing heat fluxes evaluation with loss of precision in the process.
The test bench is equipped with 3 lines of pairs of thermocouples. Those data are merged and the experimental datum presented here is the mean temperature measured for each point along with its standard deviation between the 3 lines of measurement. This gives a temperature profile on both sides (cold and hot) of the copper alloy cooled segment. A similar treatment is made on computational results to extract a mean temperature on both sides of the solid domain. The results are presented in Figure 9.

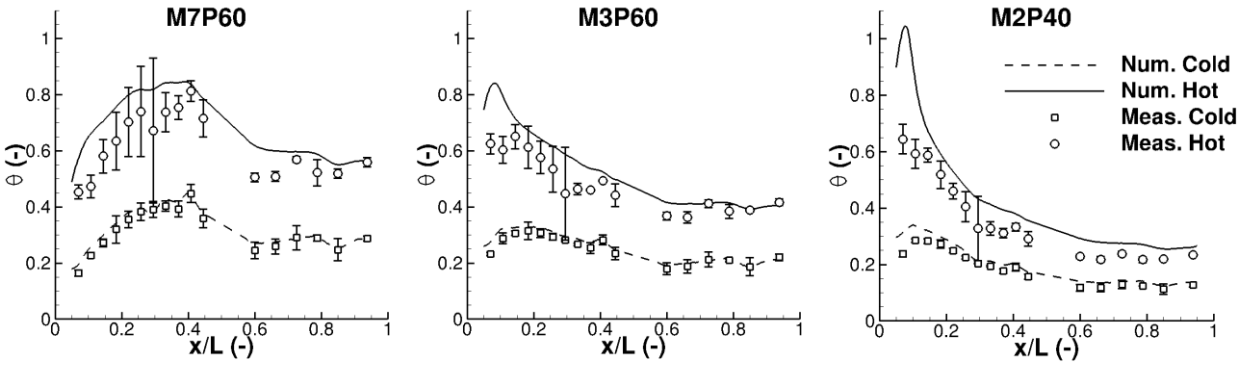

Figure 9 - Temperature profiles on both sides of the plate for the different operating conditions. Comparison to experimental measurements.

As expected, the temperature computed on the cold side of the plate matches the experimental one as this is the imposed boundary condition (with small differences due to the fact that the boundary condition is imposed at a position slightly different to the measurement plane, which is "inside" the material). The overall temperatures recovered on the hot-gas side agree very well with the experimental values, especially in a wide second part of the combustion chamber. Some discrepancies are observed, especially at the very beginning of the combustion chamber for the low-M cases. Indeed, those low-M cases correspond to high velocity ratio and shorter flames, leading to a strong recirculation zone in the combustion chamber with high temperature gases impacting the wall at the beginning of the combustion chamber. Those effects are recovered by the computation but overpredicted: this is a classical limitation of the RANS approach which is not well fitted to recover impact of heat exchanges. However, on more than 80% of the combustion chamber length, the experimental and numerical evaluations of temperatures are in very good agreement. This is really remarkable, as the temperature is a data more sensitive than the heat fluxes: if one considers the wall temperature and the heat fluxes being linked together by a relation like $\phi = h.(T_w - T_{ad})$, with no uncertainties on the heat transfer coefficient h and the adiabatic wall temperature T_{ad}, then the relative uncertainties of the heat fluxes and wall temperature can be expressed as:

$$\frac{\Delta\phi}{\phi} = \frac{\Delta T_W}{T_W - T_{ad}}$$

We can thus link the relative evolution of the heat flux to the wall temperature by:

$$\frac{\Delta\phi}{\phi} = \frac{\Delta T_W}{T_W} \cdot \frac{T_W}{T_W - T_{ad}}$$

The order of magnitude is about 500 K for the wall temperature and 3500 K for the adiabatic temperature, which gives $\Delta T_w/T_w = 6\ \Delta\phi/\phi$. This means that a 5% relative error on the heat fluxes lead to a 30% relative error on the wall temperature, which is really huge: this is illustrated in Figure 11, where the "cold side wall" boundary condition is changed from imposed experimental values to a heat transfer-water temperature condition. The computed heat fluxes are quite similar, but the change in temperature computed is greater.

The Figure 9 also exhibits a different behaviour in hot gas side temperature profiles depending on the velocity ratio. In fact, as stated before, with high velocity ratio (low mixture ratio), the flame is shorter and the recirculation zone as well. The impact of hot gases happens at the beginning of the combustion chamber. When the mixture ratio approaches the stoichiometric one, the flame is longer, leading to the hot gas zone to come near the wall later,

modifying the shape of the temperature profiles. This behaviour can be also seen in heat fluxes figures (Figure 10) where the shape of the heat fluxes profiles change with changing mixture ratio M. The computation gives overestimated heat fluxes, coherent with the overestimated temperature presented in Figure 9, but the values and the shapes of these computed heat fluxes profiles are quite in good agreement with experimental data, which is difficult to evaluate with high accuracy (as stated herebefore).

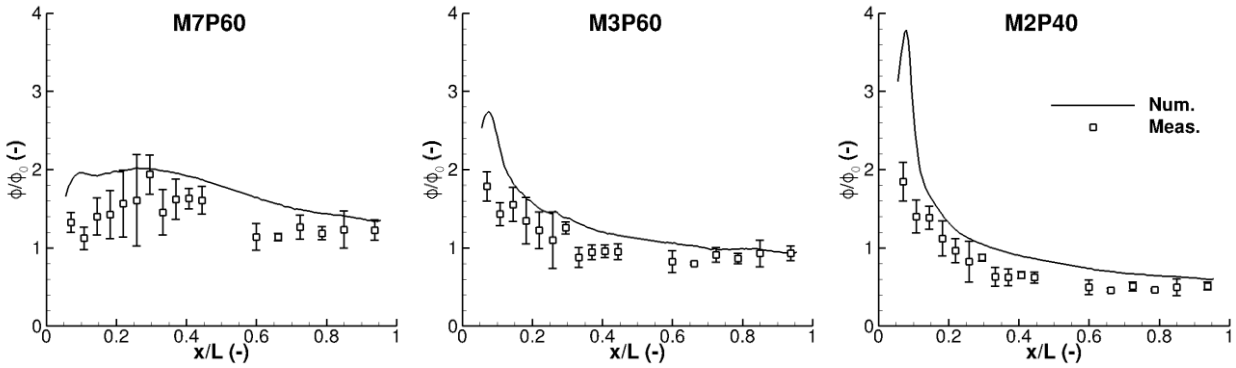

Figure 10 - Heat fluxes profiles for the different operating points computed. Comparison to experimental measurements

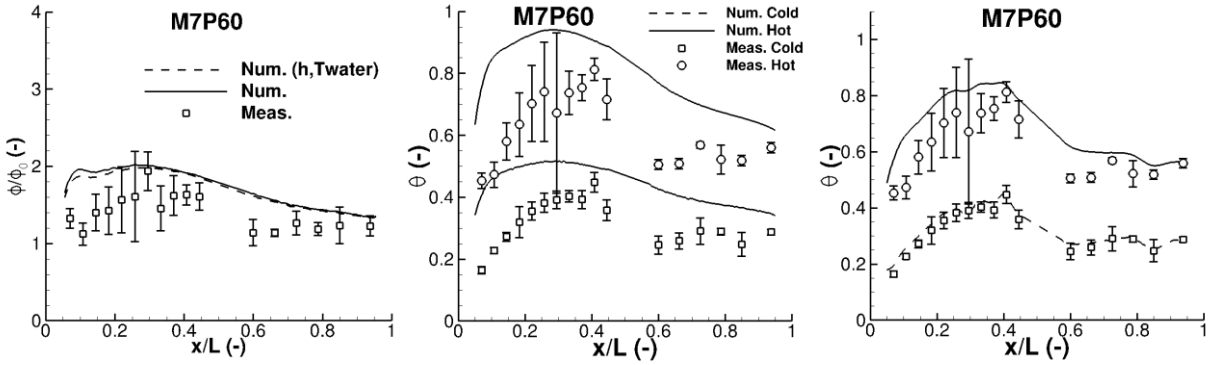

Figure 11 - Change in boundary conditions: Heat fluxes for both conditions (left), temperature profiles for (h,T_{water}) condition (middle) and cold wall temperature (right).

5. Conclusion

The water-cooled combustion chamber adapted to the cryogenic bench Mascotte, developed by Onera in partnership with the CNES has been tested during the last two years in several conditions of pressure, mixture ratio and injection temperature. Thanks to thermocouples embedded in the copper wall, temperatures were acquired near the hot gas wall and coolant wall as well, and heat fluxes were derived. The measurements have been compared, analyzed and reduced to give a first set of data for simulation with a best accuracy. Nevertheless, reflections and procedures are currently undertaken to lower those uncertainties.

RANS simulations have been performed conjugating heat transfer in the fluid and the solid. Two types of boundary conditions have been applied on the cold side: measured temperature first, and then impedance-type condition, with an estimation of the heat transfer coefficient and water temperature in the cooling channel.

The numerical results are in good agreement with experimental data, especially temperatures which are easier to compare. Indeed, due to high conductivity of copper alloy, the temperature variations in the wall are not too large leading to larger uncertainties on the fluxes compared to temperature. Nevertheless, the good comparison between numerical results and experimental measurements gives confidence in the methodology and also some areas of work.

Acknowledgments

Experimental and numerical work presented in this paper was supported by the French National Space Agency (CNES) in the frame of the common ONERA-CNES project.

References

[1] Negishi H., Daimon Y. – 2010 – Coupled Combustion and Heat Transfer Simulation for Full-Scale Regeneratively Cooled Thrust Chamber. In *Space Propulsion 2014 Conference.*

[2] Kim, S.-K., Joh, M., Choi, H.S., Park, T.S. – 2014 – Effective modeling of conjugate heat transfer and hydraulics for the regenerative cooling design of kerosene rocket engines. In *Numerical Heat Transfer; Part A: Applications*, Vol. 66, Iss. 8: 863-883

[3] Kim, S.-K., Joh, M., Choi, H. S., and Park, T. S. – 2013 – Multidisciplinary simulation of a regeneratively cooled thrust chamber of liquid rocket engine: Turbulent combustion and nozzle flow. In *International Journal of Heat and Mass Transfer*. http://www.sciencedirect.com/science/article/pii/S001793101300906X

[4] Bartolome Calvo J. , Hannemann K. – 2008 – Analysis of the Heat Transfer in Liquid Rocket Engine Cooling Channels. New Results in Numerical and Experimental Fluid Mechanics VII. In *Contributions to the 16th STAB/DGLR Symposium, Aachen, Germany*

[5] Torres Y., Stefanini L. and Suslov D. – 2009 – Influence of curvature in regenerative cooling system of rocket engine. In *3rd EUCASS*. http://dx.doi.org/10.1051/eucass/200901171

[6] Quering K., Zeiss W., Wiedmann D., Nkab O., Torres Y., Suslov D. - 2009 - Numerical and Experimental Studies of Heat Transfer in Asymmetrically Heated Cooling Channels. In *3rd EUCASS*.

[7] Masquelet M., Suresh Menon S. – 2007 - Large-Eddy Simulation of Flame-Turbulence Interactions in a Shear Coaxial Injector. In *J. of Propulsion and Power* Vol. 26, No. 5

[8] Menter, F.R. – 1994 - Two-equation eddy-viscosity turbulence models for engineering applications. In *AIAA-Journal., 32(8), pp. 1598 – 1605*.

[9] Ordonneau G., Hervat P., Vingert L., Petitot S. and Pouffary B. – 2011 – First results of heat transfer measurements in a new water-cooled combustor on the Mascotte facility. In *EUCASS Conference* , Id 144

[10] Petitot S., Vingert L., Fdida N., Grenard P., Theron M., Palerm S. - 2014 - Heat Transfer and GOX & LOX/GH2 Flame Imaging in a High-Pressure and High-Mixture Ratio rocket Combustor . In *Space Propulsion 2014 Conference*

[11] Dorey L.-H., Grenard P., Matuszewski L., Selle L. – 2014 - Experimental and numerical study of a cooled rocket combustion chamber. In *15th International Heat Transfer Conference* IHTC15-9238

[12] Conley A., Vaidyanathan A., Segal C. – 2007 – Heat Flux Measurements for a GO_2/GH_2 Single-Element Shear Injector. In *Journal of Spacecraft And Rockets Vol. 44, No. 3*

[13] Vingert L., Habiballah M., Vuillermoz P., Zurbach S. – 2000 – Mascotte, a test facility for cryogenic combustion research at high pressure. In *51st International Astronautical Congress, Rio de Janeiro.* IAF-00-S.3.06

[14] Vingert, L., Habiballah, M., and Vuillermoz, P. – 2002 – Upgrading of the Mascotte cryogenic test bench to the LOX/Methane combustion studies. In: *4th Int. Conf. on Launcher Technology*.

[15] Fdida N. et al. – 2013 – Coupling high-speed imaging diagnostics to study a LOX/GH2 flame in a high-pressure rocket combustor. In *5th EUCASS*

[16] Refloch A. et al. - 2011. - CFD Platforms and Coupling: CEDRE Software. In *The Aerospace Journal Issue 2 - March 2011*. http://www.aerospacelab-journal.org/CEDRE-Software